Progress In Electromagnetics Research M, Vol. 35, 151–161, 2014

The Research on Flux Linkage Characteristic Based on BP and RBF Neural Network for Switched Reluctance Motor

Yan Cai[1, *], Siyuan Sun[1], Chenhui Wang[1], and Chao Gao[2]

Abstract—The flux and torque of switched reluctance motor (SRM) have a highly nonlinear functional relationship with rotor position and phase current, as a consequence of the double-salient structure of the stator and rotor pole and highly magnetic saturation, which is difficult to build an accurate analytic model. In order to achieve the SRM high-performance control, it is necessary to build an accurate nonlinear model for SRM. On the basis of the adequate and precise sample data, by taking advantage of neural network that has outstanding nonlinear mapping capability, this paper adopts the Back Propagation (BP) based on Levenberg-Marquardt (LM) algorithm and Radial Basis Function (RBF) neural network to build offline models for SRM respectively. Under different requirements of model accuracy, two kinds of network are studied and compared with each other on accuracy, scale and other aspects. The research results indicate that the network scale built as SRM nonlinear model by BP neural network based on LM algorithm is smaller than the one built by RBF. Additionally, the model accuracy is higher. In terms of the Switched Reluctance Drive (SRD) which requires real-time controller, reducing the network scale will be beneficial to the online real-time control of the system.

1. INTRODUCTION

The switched reluctance motor has been applied in many fields due to its advantages including simple structure, reliable operating ability, high efficiency, low cost of manufacture and flexible control. Its double-salient structure of stator and rotor pole, highly magnetic saturation and voltage-pulse mode of power supply lead to torque ripple, noise and other disadvantages, which limit SRM's application on high-performance drive field. In order to achieve high-performance drive, it is necessary to build an accurate nonlinear model for SRM. Nevertheless, the flux linkage and torque of switched reluctance motor have a highly nonlinear functional with rotor position and phase current so that it is difficult to build an accurate analytic model.

The conventional model methods contain tabular, linear, quasi-linear, analytical expression and finite-element approaches. The tabular approach finds data through interpolation or range approximation by building a table which links current, rotor angle and flux linkage together. This approach will occupy plenty of internal memory of the CPU in controller and its accuracy is insufficient [1]. Because the linear model neglects the nonlinear feature in magnetic circuit and diffusion effect at the edge of magnetic field, it is beneficial to SRM qualitative analysis, but the model has a bigger error [2]. Roux and Morcos propose a piecewise linear method based on simplified model of flux equation. This method ignores core saturation. Compared with linear method, its accuracy has a little improvement though its error is still large [3]. By utilizing several SRM magnetization curves in important positions, SRM analytic model is built. Though its model accuracy improves compared with linear model and quasi-linear model, its error is not able to meet the requirement of model accuracy for SRM high-performance control [4]. Ilic'-Spong et al. take use of analytical expression

Received 16 January 2014, Accepted 19 March 2014, Scheduled 31 March 2014

* Corresponding author: Yan Cai (caiyan@tjpu.edu.cn).

[1] Tianjin Key Laboratory of Advance Technology of Electrical Engineering and Energy, Tianjin Polytechnic University, Tianjin 300387, China. [2] China Tex Mechanical & Electrical Engineering Ltd., Beijing 101102, China.

method to build SRM model. Even if it could optimize system performance in a certain extent, it is not adequately adaptive for various loads and environment [5]. Xu and Ruchkstater combine SRM external circuit equation and finite-element method (FEM) to simulate, which has the problems of more calculation time and plenty of data [6]. Compared with two-dimensional finite-element analysis, three-dimensional finite-element analysis has a great progress on the level of accuracy, however, its calculation is quite complicated and time-wasting. Besides, the finite-element algorithm is adapted to calculating motor performance without realizing the model requirement of SRD real-time control [7]. Sahoo et al. use tabular approach and fuzzy logic method to build current model. This method is based on the assumption that magnetic circuit is not saturated, which could not improve accuracy [8].

The difficulty of modeling for SRM is that its flux linkage characteristic is highly nonlinear. Because the neural network has good nonlinear mapping ability, its application in SRM modeling is of obvious superiority. So more and more academicians put artificial intelligence into SRM model. Elmas et al. firstly put forward building a BP neural network model for SRM by BP standard algorithm and proving its effectiveness. However, the standard BP algorithm has some problems including slow convergence speed and local minimum [9]. Cai et al. use RBF neural network based on boundary value constraint improvement to model SRM's flux linkage characteristic. The experimental results indicate that this method can provide better fitting ability, but fail to solve the problem on necessity of more neurons [10]. Fuzzy logic and neural network are combined together which could improve convergence speed. On the contrary, the network structure is more complicated and the amount of calculation is also very large [11]. Liang and Ding [12] and Xu et al. [13] use adaptive neural fuzzy inference system (ANFIS) to model for SRM. Although this method has good calculation speed and generalization ability, its network structure is too complicated to carry on motor real-time control. Si et al. use least squares support vector machine (LSSVM) to model SRM flux linkage characteristic. This model lacks prediction precision and its kernel function form and parameter choice are not theoretical and depend on experience and artificial selection [14]. Shang et al. use genetic algorithm to optimize LSSVM to improve prediction precision of the model, but this method has no sufficient data and fails to describe the motor characteristic precisely [15]. Lachman et al. compare the methods based on neural network, fuzzy logic or neural-fuzzy to model for SRM and conclude that the model built by neural network method has higher accuracy [16].

The size of network scale of SRM neural network model determines whether it can be applied in actual real-time system. Reducing the network scale is of great meaning in relieving the amount of calculation in controller for real-time system. The SRM nonlinear model is able to be trained offline, and then the trained network is used in SRD real-time control through DSP programs. Thus, to build an accurate and small-scale SRM nonlinear model is crucial to SRD which requires very high real-time performance.

This paper is based upon the sample data of flux linkage characteristic through measuring a three-phase 12/8 SRM prototype motor [17]. The research is done on offline model for SRM flux linkage characteristic respectively by adopting BP neural network based on improved algorithm and RBF neural network. Under different requirements of model accuracy, two kinds of network are studied and compared with each other at accuracy, scale and other aspects. The research results indicate that adopting BP or RBF neural network to build SRM flux model has a higher accuracy, and increasing the number of neurons properly can improve the precision. If the neurons in hidden layer are identical, the accuracy of BP model is higher than RBF. In addition, compared with RBF neural network, the SRM model of BP neural network based on improved algorithm has smaller network scale, which is good for SRM real-time system to operate.

2. THE FLUX LINKAGE CHARACTERISTIC OF SRM AND ITS SAMPLE ACQUIREMENT

2.1. The Mathematic Model for SRM

SRM is variable-reluctance brushless motor with stator-rotor double-salient structure. The rotor poles have neither windings nor permanent magnet. There are concentrated windings on the stator poles. The motor current and flux linkage serve as unidirectional pulses changing with time. Its air-gap magnetic field is pulsatile. Due to such a geometrical structure and the nonlinear characteristic of magnetic

circuit, the winding inductance and flux linkage in SRM are both nonlinear function with current and rotor position.

According to basic circuit law and regardless of magnetic hysteresis and vortex and mutual inductance between windings, the voltage balance equation in the j-th winding in SRM is shown as

$$\mathbf{U}_j = \mathbf{R}_j \mathbf{i}_j + \frac{\mathbf{d}\boldsymbol{\psi}_j}{\mathbf{dt}} \tag{1}$$

where $\mathbf{U}_j$, $\mathbf{R}_j$, $\mathbf{i}_j$, $\boldsymbol{\psi}_j$ respectively stand for phase voltage, phase resistor, phase current and flux linkage in the j-th stator windings. j is the number of phases.

According to the principle of motor, the electromagnetic torque produced by each winding in SRM is able to be expressed as magnetic co-energy's partial derivative towards rotor position angle. That is

$$\mathbf{T}_j = \left.\frac{\partial \mathbf{W}'_j}{\partial \boldsymbol{\theta}}\right|_{i=\text{const}} = \frac{\partial \int_0^{i_j} \boldsymbol{\psi}_j (\mathbf{i}_j, \boldsymbol{\theta}) \mathbf{di}_j}{\partial \boldsymbol{\theta}} \tag{2}$$

The whole electromagnetic torque is the sum of torque in each phase winding

$$\mathbf{T}_e = \sum\nolimits_{j=1}^{m} \mathbf{T}_j(\mathbf{i}_j, \boldsymbol{\theta}) \tag{3}$$

According to the laws of mechanics, the rotor mechanic motion equation is concluded as

$$\mathbf{T}_e = \mathbf{J}\frac{\mathbf{d}^2\boldsymbol{\theta}}{\mathbf{dt}^2} + \mathbf{D}\frac{\mathbf{d}\boldsymbol{\theta}}{\mathbf{dt}} + \mathbf{T}_L \tag{4}$$

where $\mathbf{T}_e$, $\mathbf{T}_L$, $\mathbf{J}$, $\mathbf{D}$ respectively stand for electromagnetic torque, load torque, rotary inertia and friction factor.

Although the mathematical model of SRM mentioned above describes the electromagnetic and mechanic relation in theory completely and accurately, it is difficult for SRM to solve exactly by analysis formulas because of its highly nonlinear characteristic of flux linkage.

2.2. The Acquirement of Flux Sample Data

Considering that neural network has excellent nonlinear mapping ability, this paper adopts neural network to model for SRM flux linkage characteristic. In order to build an accurate model, acquiring sufficient and precise training data is indispensable for network training. So, it firstly needs precise flux linkage detection. The SRM flux detection can be divided into two methods that contain direct detection and indirect detection. The direct detection method measures flux linkage directly by flux sensor which must be installed when motor is assembled. It causes higher cost and more complicated structure. Additionally, the measuring range of the flux sensor is limited. These problems above restrict its practical application. The indirect detection method is that through adding a DC voltage suddenly on a certain winding and measuring the voltage and current value in transient process, the flux linkage is obtained by integrating transformation form of voltage balance Equation (1), the formula is as below.

$$\boldsymbol{\psi}_j (\mathbf{t}) = \int_0^t [\mathbf{U}_j (\mathbf{t}) - \mathbf{R}_j \mathbf{I}_j (\mathbf{t})] \mathbf{dt} + \boldsymbol{\psi}_j (0) \tag{5}$$

By discretizing Equation (5),

$$\boldsymbol{\psi}_j (\mathbf{k}) = \left\{ \sum\nolimits_{k=1}^{N} [\mathbf{U}_j (\mathbf{k}) - \mathbf{R}_j \mathbf{I}_j (\mathbf{k})] \boldsymbol{\Delta} \mathbf{t} \right\} + \boldsymbol{\psi}_j (0) \tag{6}$$

where $\boldsymbol{\psi}_j(0)$ is the initial flux value.

From Formula (6), the flux value can be obtained by measuring each transient voltage and current. This paper uses the indirect detection method to measure the flux linkage. It takes advantage of digital signal processor (DSP) because of its short sampling interval so as to cut down sampling period and realize measuring flux linkage characteristic precisely.

The prototype motor is a 1.5 kW three-phase 12/8 SRM. Its flux linkage change cycle is 45°. Considering that flux linkage is symmetrical in accordance with stator-and-rotor salient aligned position, it just needs to measure the flux linkage in half of a cycle (0°–22.5°). In order to guarantee well-distributed flux sample, the voltage and current data are collected respectively in every 1° degree. The maximum of measured current is higher than actual operating current, which assures that sample set covers the whole operating area.

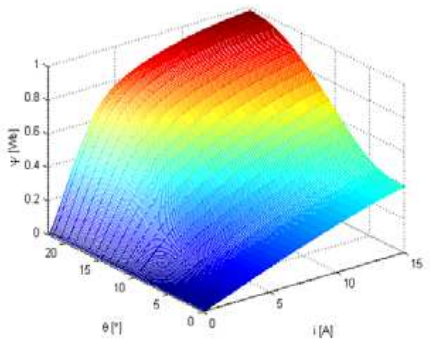

Figure 1. The actual measured magnetization curve.

2.3. The Analysis on Magnetization Curve

The magnetization characteristic through actual measurement is shown in Figure 1, and the flux linkage has a nonlinear function with rotor position and phase current. The characteristics are as follow.

(1). When the central line of the stator salient pole is aligned with the central line of rotor groove ($\boldsymbol{\theta} = 0°$), the relation between the flux linkage and current is linear.

(2). When the central lines of the stator and rotor poles are aligned ($\boldsymbol{\theta} = 22.5°$), the air gap is so narrow that the saturation degree of magnetization curve is the highest.

(3). The flux linkage is periodic to rotor position. That is

$$\boldsymbol{\psi}\left(\mathbf{i}, \boldsymbol{\theta} + \frac{2\boldsymbol{\pi}}{\mathbf{N}_r}\right) = \boldsymbol{\psi}(\mathbf{i}, \boldsymbol{\theta}) \tag{7}$$

And the magnetization curve in each cycle is symmetric to the aligned position of salient poles of stator and rotor.

$$\boldsymbol{\psi}\left(\mathbf{i}, \left(\frac{2\boldsymbol{\pi}}{\mathbf{N}_r} - \boldsymbol{\theta}\right)\right) = \boldsymbol{\psi}(\mathbf{i}, \boldsymbol{\theta}) \tag{8}$$

where $\mathbf{N}_r$ is the number of rotor poles.

(4). When phase current is fixed, from the aligned position of stator salient pole and rotor groove to the aligned position of stator and rotor salient poles, the flux linkage is kept increasing monotonically. That is

$$\boldsymbol{\psi}(\mathbf{i}, \boldsymbol{\theta}_2) > \boldsymbol{\psi}(\mathbf{i}, \boldsymbol{\theta}_1) \quad 0° \le \boldsymbol{\theta}_1 \le \boldsymbol{\theta}_2 \le \frac{\boldsymbol{\pi}}{\mathbf{N}_r} \tag{9}$$

From the aligned position of stator and rotor salient poles to the next aligned position of stator salient pole and rotor groove, the flux linkage is kept decreasing monotonically. That is

$$\boldsymbol{\psi}(\mathbf{i}, \boldsymbol{\theta}_2) < \boldsymbol{\psi}(\mathbf{i}, \boldsymbol{\theta}_1) \quad \frac{\boldsymbol{\pi}}{\mathbf{N}_r} \le \boldsymbol{\theta}_1 \le \boldsymbol{\theta}_2 \le \frac{2\boldsymbol{\pi}}{\mathbf{N}_r} \tag{10}$$

(5). When rotor is fixed on a certain position, the flux linkage $\boldsymbol{\psi}$ is increasing monotonically with phase current $\mathbf{i}$. That is

$$\boldsymbol{\psi}(\mathbf{i}_1, \boldsymbol{\theta}) > \boldsymbol{\psi}(\mathbf{i}_2, \boldsymbol{\theta}) \quad \mathbf{i}_1 > \mathbf{i}_2 \tag{11}$$

(6). To each rotor position, when winding current is low, flux linkage is close to a linear relation with current and when winding current is high, which is not at the aligned position of the two central lines of stator salient pole and rotor groove, flux linkage appears nonlinear.

3. THE ESTABLISHMENT OF MAGNETIC MODEL BASED ON BP NEURAL NETWORK

BP neural network is an error-back-propagation multi-layer feedforward network. Generally, it contains input layer, hidden layer and output layer. Input layer neurons are linear, whereas neurons in the hidden

layers have sigmoidal signal functions and output layer neurons are linear or sigmoidal. Standard BP is a gradient descent algorithm, as the Widrow-Hoff learning rule, in which the network weights are moved along the negative of the gradient of the performance function. Its error is propagated back layer by layer to revise the weight value between layers. The adjusting process is as follow.

The formulae that adjust weights in output layer are

$$\boldsymbol{\Delta}\mathbf{w}_{kj}^{2} = -\boldsymbol{\eta}\frac{\partial \mathbf{E}}{\partial \mathbf{w}_{kj}^{2}} = \boldsymbol{\eta}\cdot\boldsymbol{\delta}_{kj}\cdot\mathbf{a}_{j}^{1} \tag{12}$$

$$\mathbf{w}_{kj}^{2}(\mathbf{n}+1) = \mathbf{w}_{kj}^{2}(\mathbf{n}) + \Delta\mathbf{w}_{kj}^{2} \tag{13}$$

$$\boldsymbol{\delta}_{kj} = \left(\mathbf{t}_{k} - \mathbf{a}_{k}^{2}\right)\cdot\mathbf{f}_{2}' = \mathbf{e}_{k}\cdot\mathbf{f}_{2}' \tag{14}$$

where $\mathbf{w}_{kj}^{2}$ is the weight from j-th input to k-th output, $\mathbf{E}$ the network error, $\mathbf{a}_{j}^{1}$ the j-th output in hidden layer, $\mathbf{t}_{k}$ the expected output, $\mathbf{a}_{k}^{2}$ the network output, and $\mathbf{f}_{2}'$ the derivative of the transfer function in output layer.

The formulae that adjust weight in hidden layer are

$$\boldsymbol{\Delta}\mathbf{w}_{ji}^{1} = -\boldsymbol{\eta}\frac{\partial \mathbf{E}}{\partial \mathbf{w}_{ji}^{1}} = \boldsymbol{\eta}\cdot\boldsymbol{\delta}_{ji}\cdot\mathbf{p}_{i} \tag{15}$$

$$\mathbf{w}_{ji}^{1}(\mathbf{n}+1) = \mathbf{w}_{ji}^{1}(\mathbf{n}) + \boldsymbol{\Delta}\mathbf{w}_{ji}^{1} \tag{16}$$

$$\boldsymbol{\delta}_{ji} = \mathbf{e}_{j}\cdot\mathbf{f}_{1}' = \sum\nolimits_{k=1}^{s^{2}}\boldsymbol{\delta}_{kj}\cdot\mathbf{w}_{kj}^{2}\cdot\mathbf{f}_{1}' \tag{17}$$

where $\mathbf{w}_{ji}^{1}$ is the output weight from i-th input to j-th output, $\mathbf{p}_{i}$ the i-th network input, and $\mathbf{f}_{1}'$ the derivative of the transfer function in hidden layer.

BP neural network can achieve any nonlinear mapping from input to output and has self-learning ability and generalization ability. But BP neural network has problems of slow convergence speed and local minimum. In order to overcome the problem of slow convergence speed, many improved algorithms have been proposed. Conjugate gradient algorithm is a kind of improved gradient methods which can relieve the oscillation and bad convergence. In the conjugate gradient algorithms, a search is performed along conjugate directions, which produces generally faster convergence than gradient descent directions. In the conjugate gradient algorithm, the step size is adjusted at each iteration, which is a waste of time. Newton's method is an alternative to the conjugate gradient methods for fast optimization. It often converges faster than conjugate gradient methods. Unfortunately, it is complex and expensive to compute the Hessian matrix for feedforward neural networks. Quasi-Newton algorithm which is adopted on the basis of Newton algorithm is one that need not calculate second-order derivative matrix and its inverse matrix. The basic idea of Quasi-Newton is to use gradient information or approximate matrix to replace Hessian matrix. It not only need not calculate second-order derivative, but also carries on approximation well so that the fast convergence speed is kept and avoids complicated calculation in Newton's method. However, considering that it is inevitable to save a n-dimensional approximate Hessian matrix, it occupies more internal memory. As a consequence, Quasi-Newton algorithm is limited to use in small-scale neural network design. When the performance function has the form of a sum of squares, adopting LM algorithm can avoid calculating Hessian matrix and its inverse matrix. The LM algorithm uses this approximation to the Hessian matrix in the following Newton-like update:

$$\mathbf{w}(\mathbf{n}+1) = \mathbf{w}(\mathbf{n}) - \left(\mathbf{J}^{T}\mathbf{J} + \boldsymbol{\mu}\mathbf{I}\right)^{-1}\mathbf{J}^{T}\mathbf{E} \tag{18}$$

where $\mathbf{J}$ is Jacobian matrix, $\mathbf{E}$ the network error vector, $\boldsymbol{\mu}$ a certain nonnegative number that can be self-adaptive, and $\mathbf{I}$ the unit matrix.

When the scalar $\boldsymbol{\mu}$ is zero, this is just Newton's method, using the approximate Hessian matrix. When $\boldsymbol{\mu}$ is large, this becomes gradient descent with a small step size. LM algorithm combines the fast speed derived from Newton's method and convergence characteristic from gradient descent method. The number of its iterations during converging is fewer but the amount of calculation in each iterative step is large. Owing to the smaller network scale of BP in SRM, it is suitable to use LM algorithm as an optimized algorithm.

Focusing on the local minimum existing in BP algorithm, this paper uses several groups of different initial conditions to train the network and picks out the best result in order to make errors low enough

to be accepted. For the sake of a better generalization in the network, on the basis of accurate sample data, the uniform process is carried out, and the aberrant point is removed. It classifies the data as sample set and test set. The data in test set are used for verification.

When training target is set as 0.001, the network structure of magnetic characteristic through actual training is shown in Figure 2. This is a BP neural network with dual input, single output and single hidden layer. There are two neurons in hidden layer. The input variables are the rotor angle position $\boldsymbol{\theta}$ and current $\mathbf{i}$ in phase windings, both of which are uniformed through $\mathbf{k}_1$, $\mathbf{k}_2$ and then added in the network. The output is flux linkage $\boldsymbol{\psi}$.

The output of unit j in hidden layer is:

$$\mathbf{a}_j^1 = \mathbf{f}_1\left(\sum_{i=1}^{2} \mathbf{w}_{ji}^1 \cdot \mathbf{x}_i + \mathbf{b}_j^1\right) \quad j = 1, 2 \tag{19}$$

where $\mathbf{w}_{ji}^1$ is the weight from input unit $\mathbf{x}_i$ $(i = 1, 2)$ to hidden layer unit $\mathbf{a}_j^1$, and $\mathbf{b}_j^1$ is the threshold value. The activation function $\mathbf{f}_1$ in hidden layer is tansig function.

$$\mathbf{f}_1(\mathbf{x}) = \frac{1 - \mathbf{e}^{-2x}}{1 + \mathbf{e}^{-2x}} \tag{20}$$

The output of unit in output layer is:

$$\mathbf{y} = \mathbf{f}_2\left(\sum_{j=1}^{2} \mathbf{w}_{1j}^2 \cdot \mathbf{a}_j^1 + \mathbf{b}^2\right) \tag{21}$$

where $\mathbf{w}_{1j}^2$ is the weight from hidden layer unit $\mathbf{a}_j^1$ to output layer $\mathbf{y}$ and $\mathbf{b}^2$ the threshold value.

The activation function $\mathbf{f}_2$ in output layer is a linear function.

$$\mathbf{f}_2(\mathbf{x}) = \mathbf{x} \tag{22}$$

Define the target error function as:

$$\mathbf{E}(\mathbf{t}) = \frac{1}{2}\sum_{k=1}^{P} [\mathbf{t}_k - \mathbf{y}_k(\mathbf{t})]^2 \tag{23}$$

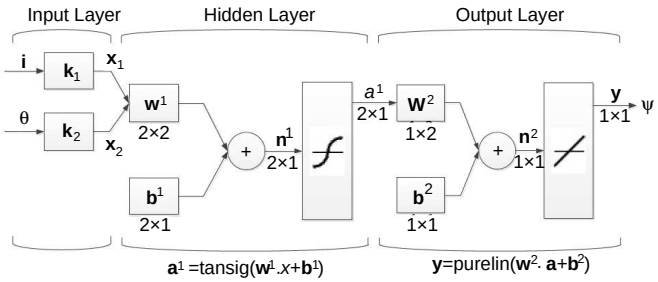

Figure 2. The BP neural network structure of magnetic characteristic.

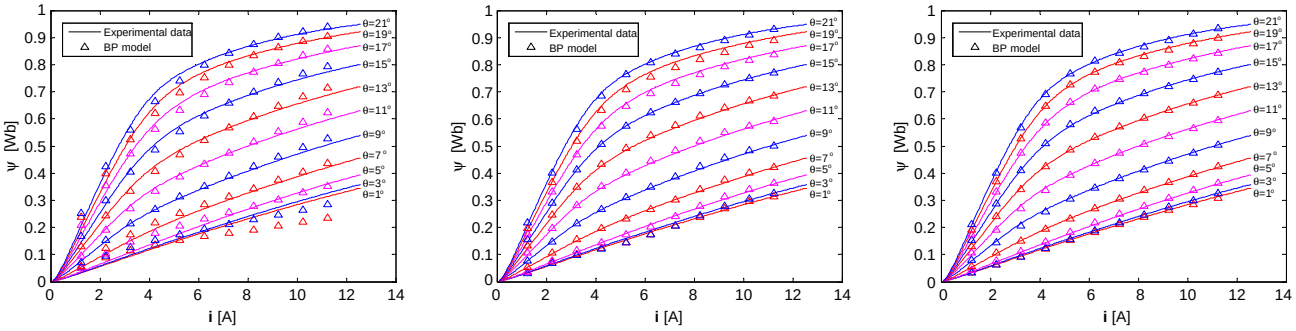

Figure 3. Comparison between BP model under different target accuracy and experimental data, Figures (a), (b), (c) represent that the target accuracy is 0.001, 0.0001, 0.00002 respectively.

where $\mathbf{t}_k$ is the desired output, $\mathbf{y}_k(\mathbf{t})$ the output through network calculation, and $\mathbf{P}$ the number of training sample data.

When the number of neurons in hidden layer is 2, its model accuracy is $5.60*10^{-4}$. The comparison result between the BP neural network model of SRM and flux linkage data through actual measurement is shown in Figure 3(a). In order to improve the accuracy of the model, it adopts the method of adding neurons in hidden layer. When the number of neurons in hidden layer is 4 and 6, respectively, their model accuracy is $8.84*10^{-5}$ and $1.95*10^{-5}$. The comparison result between the model and flux linkage data through actual measurement is shown in Figure 3(b) and Figure 3(c). From the figure, increasing the number of neurons in hidden layer is able to improve the level of accuracy. Evidently, the SRM nonlinear model built by BP neural network has high precision and small scale.

4. THE ESTABLISHMENT OF MAGNETIC MODEL BASED ON RBF NEURAL NETWORK

RBF neural network is a three-layer feedforward neural network with excellent performance. In the structure, the input and output layer neurons are linear. The hidden layer often adopts Gauss function. The output unit carries on linear weighting from the hidden units so as to achieve mapping from input space to output space so that the whole network can reach the goal of function approximation. RBF can require more neurons than BP networks, but often they can be designed in a fraction of the time it takes to train standard feedforward networks.

The network structure of magnetic characteristic by RBF neural network training is shown in Figure 4. This is a network with dual input and single output. The number of hidden layer neurons is 6, and the input variables are rotor position $\boldsymbol{\theta}$ and current $\mathbf{i}$ in phase windings, both of which are uniformed through $\mathbf{k}_1$, $\mathbf{k}_2$ and then added in the network. The output is flux linkage $\boldsymbol{\psi}$.

The output of unit j in hidden layer is:

$$\mathbf{a}_j^1 = \mathbf{f}_1\left(\left\|\mathbf{w}_{ji}^1 - \mathbf{x}_i\right\| \cdot \mathbf{b}_j^1\right) \quad j = 1, 2, 3, 4, 5, 6 \tag{24}$$

where $\|\mathbf{w}_{ji}^1 - \mathbf{x}_i\| = \sqrt{\sum_{i=1}^{2}\left(\mathbf{w}_{ji}^1 - \mathbf{x}_i\right)^2}$ is called Euclidean distance. $\mathbf{w}_{ji}^1$ is the weight from input unit $\mathbf{x}_i$ $(i = 1, 2)$ to hidden layer unit $\mathbf{a}_j^1$. The threshold $\mathbf{b}_j^1$ can adjust the function's sensitivity. The transfer function $\mathbf{f}_1$ in hidden layer is Gauss function.

$$\mathbf{f}_1(\mathbf{x}) = \mathbf{e}^{-x^2} \tag{25}$$

The output of unit in output layer is:

$$\mathbf{y} = \mathbf{f}_2\left(\sum\nolimits_{j=1}^{6} \mathbf{a}_j^1 \cdot \mathbf{w}_{1j}^2 + \mathbf{b}^2\right) \tag{26}$$

where $\mathbf{w}_{1j}^2$ is the weight from hidden layer unit $\mathbf{a}_j^1$ to output $\mathbf{y}$ and $\mathbf{b}^2$ the threshold value. The transfer function $\mathbf{f}_2$ in output layer is a linear function.

$$\mathbf{f}_2(\mathbf{x}) = \mathbf{x} \tag{27}$$

Based on SRM flux linkage model of RBF neural network, when the number of neurons in hidden layer is 6, its model accuracy is $7.92 * 10^{-4}$. The comparison result between the RBF neural network

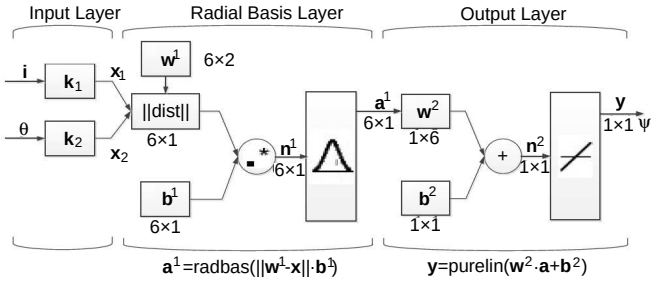

Figure 4. The RBF neural network structure of magnetic characteristic.

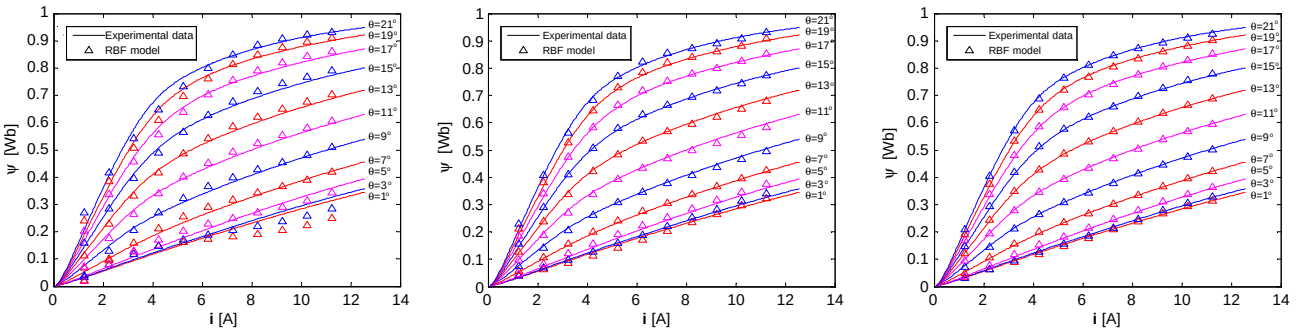

Figure 5. Comparison between RBF model under different target accuracy and experimental data, Figures (a), (b), (c) represents that the target accuracy is 0.001, 0.0001, 0.00002 respectively.

model and flux linkage data through actual measurement is shown in Figure 5(a). To build SRM flux linkage model based on RBF neural network, adding neurons in hidden layer can also improve the accuracy of the model. When the number of neurons in hidden layer is 10 and 15, their accuracy is $9.20 * 10^{-5}$ and $1.98 * 10^{-5}$. The comparison result between the RBF neural network model and flux linkage data through actual measurement is shown in Figure 5(b) and Figure 5(c).

5. THE CONTRAST BETWEEN THESE TWO APPROACHES FOR SRM MODEL

This paper carries out a model research with different levels of accuracy respectively based on BP of optimized algorithm and RBF neural network. Additionally, it takes mean square error (MSE) and correlation coefficient of linear regression as the evaluating indicator that judges the accuracy. Then, the model built by neural network is compared with experimental data to verify its precision.

MSE is mean square error and refers to the desired value that is the square of difference of estimated value and true value, which is a convenient way to measure mean error and is able to evaluate data's variety degree. The smaller MSE is, the closer the correlation coefficient gets to 1, the more precise the experimental data that network model describes are.

$$\mathrm{MSE} = \frac{1}{\mathbf{N}} \sqrt{\sum\nolimits_{\mathrm{i}=1}^{N} \left(\mathbf{T}\left(\mathbf{i}\right) - \mathbf{E}\left(\mathbf{i}\right)\right)^2} \tag{28}$$

where $\mathbf{T}(\mathbf{i})$ is the true value and $\mathbf{E}(\mathbf{i})$ is estimated value.

When target accuracy is 0.001, 0.0001 and 0.00002 respectively, the neurons and model accuracy of SRM flux linkage model by adopting BP and RBF are listed in Table 1.

The error curves of BP and RBF neural network during training are shown in Figure 6 and Figure 7. From the figure, we can understand that with the neurons increasing, the time that network needs to

Table 1. The comparison of flux linkage model between BP and RBF neural network under different target accuracy.

Target accuracy	Network style	Neurons in hidden layer	MSE	Correlation coefficient
0.001	BP	2	$5.60 * 10^{-4}$	0.99649
	RBF	6	$7.92 * 10^{-4}$	0.99613
0.0001	BP	4	$8.84 * 10^{-5}$	0.9996
	RBF	10	$9.20 * 10^{-5}$	0.9995
0.00002	BP	6	$1.95 * 10^{-5}$	0.9999
	RBF	15	$1.98 * 10^{-5}$	0.9999

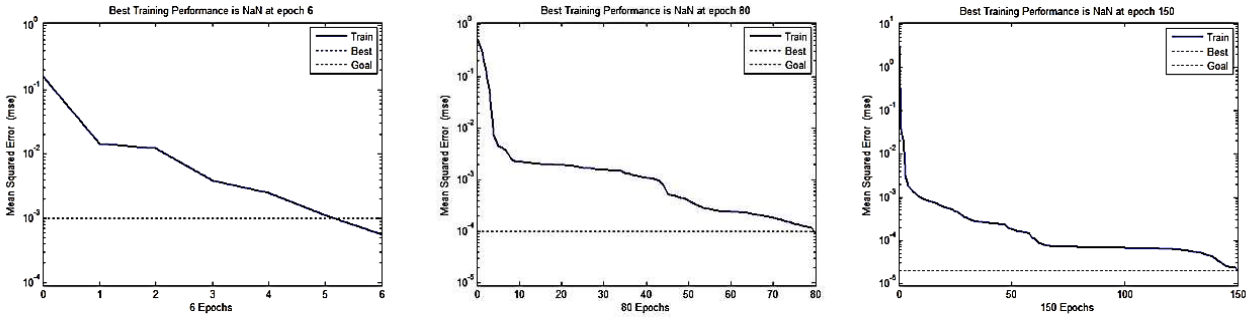

Figure 6. The error curves of BP neural network training under different target accuracy. (a) When the goal is 0.001. (b) When the goal is 0.0001. (c) When the goal is 0.00002.

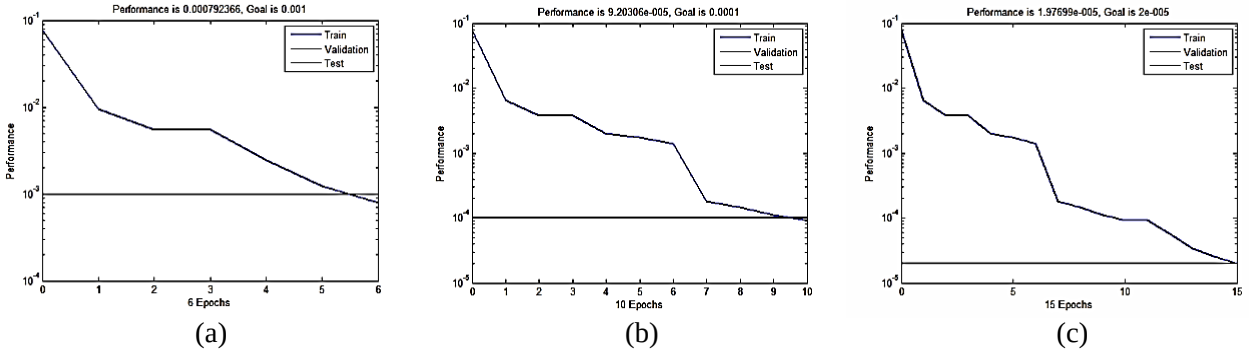

Figure 7. The error curves of RBF neural network training under different target accuracy. (a) When the goal is 0.001. (b) When the goal is 0.0001. (c) When the goal is 0.00002.

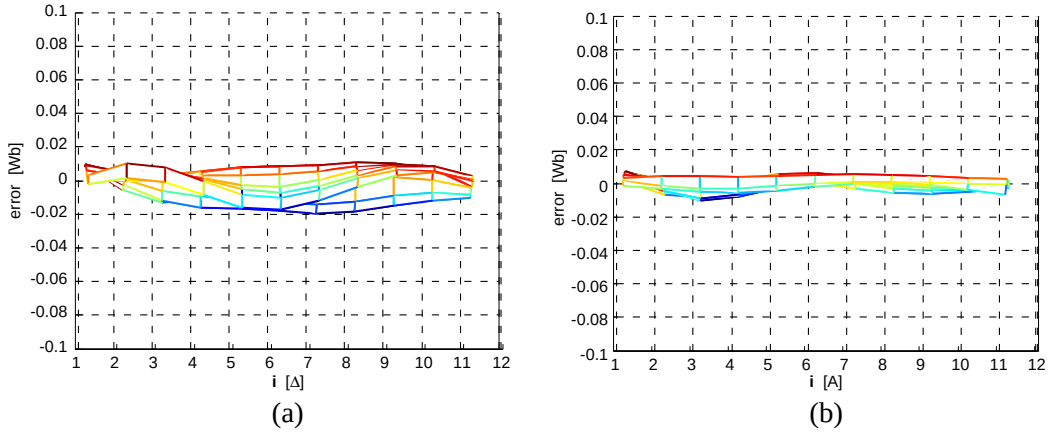

Figure 8. The error curves of BP model when the hidden neurons are 4 and 6. (a) When the hidden neurons are 4. (b) When the hidden neurons are 6.

train is increasing. On the whole, the training time that RBF takes is much less than the time that BP takes.

When BP network adopts 4 and 6 neurons, respectively, and RBF network adopts 6 and 10 neurons, the errors between the model built by neural network and experimental data are shown in Figure 8 and Figure 9. The maximum errors are 0.0194 Wb, 0.0104 Wb and 0.0654 Wb, 0.0208 Wb correspondingly. From the figures, when the neurons in hidden layer are identical (e.g., both are 6), the accuracy of BP network is higher than RBF. When the neurons in hidden layer adopted by BP network are 4, the model

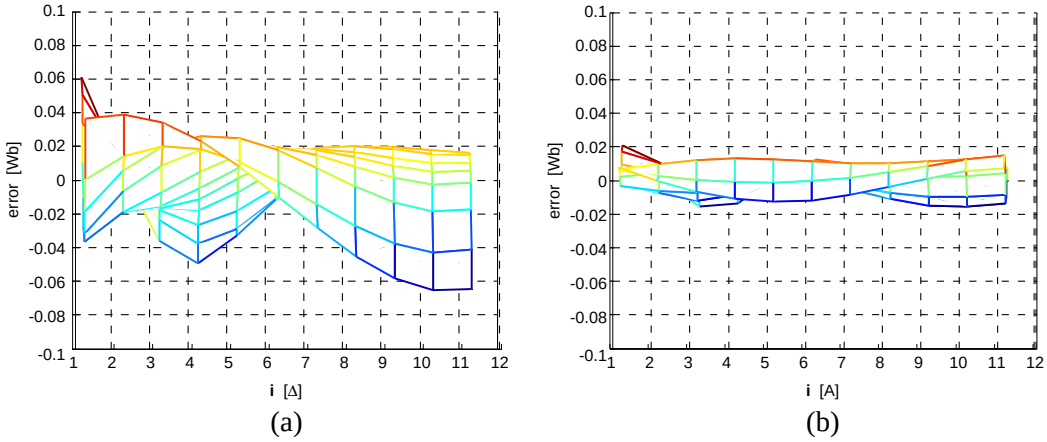

Figure 9. The error curves of RBF model when the hidden neurons are 6 and 10. (a) When the hidden neurons are 6. (b) When the hidden neurons are 10.

accuracy is higher than that built by RBF network when its neurons in hidden layer are 6. When the neurons in hidden layer adopted by BP network are 6 compared with RBF that adopts 10 neurons in hidden layer, the same conclusion can also be drawn. Evidently, modeling by BP network based on LM algorithm has smaller network scale and higher model accuracy than modeling by RBF network.

By the comparison between BP and RBF neural networks used to build flux model, there are conclusions below:

(1). Increasing the number of neurons in hidden layer can improve the model accuracy, whether using BP or RBF neural network. Moreover, the number of added neurons in hidden layer should be suitable. Maybe, adding excessive neurons will lead to over-fitting phenomenon.

(2). In terms of building SRM flux linkage model, if the numbers of neurons in hidden layer are equal, BP has higher accuracy than RBF.

(3). The convergence rate of RBF training is fast, and it has the only best approximation property. That is, if one uncertain nonlinear function f is given, there is one set of weights that can always be found and that make regularization network better than other possible choices for f approximation.

(4). If the levels of accuracy are identical, the network scale of BP neural network is smaller than that of RBF neural network, which is convenient for real-time control.

In brief, both BP neural network and RBF neural network can be used to build SRM model, and the training time that RBF uses is much less than BP. However, even if the improved algorithm is adopted, the number of units in hidden layer in RBF neural network is much larger than the units in BP neural network that takes sigmoidal function. This is because radial basis function is a local approximation. Its input space is little and only responses in smaller range. The bigger the input range is (the more input data groups or wider variation range), the more neurons RBF needs. Nevertheless, sigmoidal function is a global approximation network and can response to the whole input space. It is the global approximation performance that makes it readjust weight in each layer during every sample iteration, which slows down the convergence speed. Thus, the network scale of the SRM model built by BP neural network based on optimizing algorithm is smaller than the SRM model built by RBF neural network. The BP neural network model with the property of small scale and high accuracy is more suitable for the requirement of real-time control.

6. CONCLUSION

This paper carries out a model research offline on SRM flux linkage characteristic respectively adopting BP based on optimizing algorithm and RBF neural network. The research results present that the BP neural network based on the LM improved algorithm has advantages in model accuracy and scale.

Although RBF has the only best approximation property and its convergence rate is fast, its network scale is larger than BP. The BP neural network model with small scale and high accuracy is beneficial to SRM's real-time control.

ACKNOWLEDGMENT

This work was supported by the National Natural Science Foundation of China under grand No. 51077100.

REFERENCES

1. Stephenson, J. M. and J. Corda, "Computation of torque and current in doubly salient reluctance motors from nonlinear magnetization data," *IEE Proceedings*, Vol. 126, No. 5, 393–396, 1979.
2. Chi, H. P., R. L. Lin, and J. F. Chen, "Simplified flux linkage model for switched reluctance motors," *IEE Proceedings of Electrical Power Application*, Vol. 152, No. 3, 577–583, 2005.
3. Roux, C. and M. M. Morcos, "A simple model for switched reluctance motors," *IEEE Power Engineering Review*, Vol. 20, No. 10, 49–52, 2000.
4. Xue, X. D., K. W. E. Cheng, S. L. Ho, and K. F. Kwok, "Trigonometry-based numerical method to compute nonlinear magnetic characteristics in switched reluctance motors," *IEEE Transactions on Magnetics*, Vol. 43, No. 4, 1845–1848, 2007.
5. Ilic'-Spong, M., R. Marino, S. M. Peresada, and D. Taylor, "Feedback linearizing control of switched reluctance motors," *IEEE Transactions on Automation Control*, Vol. 32, No. 5, 371–379, 1987.
6. Xu, L. and E. Ruchkstater, "Direct modeling of switched reluctance machine by coupled field-circuit method," *IEEE Transactions Energy Conversion*, Vol. 10, No. 3, 446–454, 1995.
7. Sun, Y., J. Wu, and Q. Xiang, "The mathematic model of bearingless switched reluctance motor based on the finite-element analysis," *Proceedings of the CSEE*, Vol. 27, No. 12, 33–40, 2007.
8. Sahoo, N. C., S. K. Panda, and P. K. Dash, "A fuzzy logic based current modulator for torque ripple minimization in switched reluctance motors," *Electric Machines and Power Systems*, Vol. 27, No. 2, 181–194, 1999.
9. Elmas, C., S. Sagiroglu, I. Colak, and G. Bal, "Modeling of a nonlinear switched reluctance drive based on artificial neural networks," *Power Electronics and Variable-Speed Drives*, 7–12, 1994.
10. Cai, J., Z. Q. Deng, R. Y. Qi, Z. Y. Liu, and Y. H. Cai, "A novel BVC-RBF neural network based system simulation model for switched reluctance motor," *IEEE Transactions on Magnetics*, Vol. 47, No. 4, 830–838, 2011.
11. Xiu, J., C. Xia, and S. Wang, "Modeling of switched reluctance motor based on pi-sigma fuzzy neural network," *Transactions of China Electrotechnical Society*, Vol. 24, No. 8, 46–64, 2009.
12. Liang, D. and W. Ding, "Modeling and predicting of a switched reluctance motor drive using radial basis function network-based adaptive fuzzy system," *IET Electric Power Applications*, Vol. 3, No. 3, 218–230, 2009.
13. Xu, A., Y. Fan, and Z. Li, "Modeling of switched reluctance motor based on GA-ANFIS," *Electric Machines and Control*, Vol. 15, No. 7, 54–59, 2011.
14. Si, L., H. Lin, and Z. Liu, "Modeling of switched reluctance motors based on LS-SVM," *Proceedings of the CSEE*, Vol. 27, No. 6, 26–30, 2007.
15. Shang, W., S. Zhao, and Y. Shen, "Application of LSSVM optimized by genetic algorithm to modeling of switched reluctance motor," *Proceedings of the CSEE*, Vol. 29, No. 12, 65–69, 2009.
16. Lachman, T., T. R. Mohamad, and C. H. Fong, "Nonlinear modeling of switched reluctance motors using artificial intelligence techniques," *IEE Proceedings of Electrical Power Application*, Vol. 151, No. 1, 53–60, 2004.
17. Cai, Y., Z. Xu, and C. Gao, "Building of a nonlinear model of switched reluctance motor by BP neural networks," *Journal of Tianjin University*, Vol. 38, No. 10, 869–873, 2005.